Vol.64: e21200795, 2021
https://doi.org/10.1590/1678-4324-75years-2021200795
ISSN 1678-4324 Online Edition

Article - 75 years - Special Edition

Optimized Chitosan-Coated Gliadin Nanoparticles Improved the Hesperidin Cytotoxicity over Tumor Cells

Irineo Kelte Filho[1]
https://orcid.org/ 0000-0001-9873-2653

Celso Vataru Nakamura[2]
https://orcid.org/ 0000-0002-9911-7369

Christiane Schineider Machado[1]
https://orcid.org/ 0000-0003-1619-8667

Najeh Maissar Khalil[1]
https://orcid.org/ 0000-0002-5140-9944

Camila Diedrich[1]
https://orcid.org/ 0000-0002-3549-2952

Rubiana Mara Mainardes[1]*
https://orcid.org/ 0000-0002-4442-2075

Thaysa Ksiaskiewcz Karam[2]
https://orcid.org/ 0000-0002-3380-7922

[1]Midwestern Paraná State University, Pharmaceutical Nanotechnology Laboratory, Guarapuava, Paraná, Brazil. [2]State University of Maringá, Laboratory of Technological Innovation in the Development of Drugs and Cosmetics, Maringá, Paraná, Brazil.

Editor-in-Chief: Alexandre Rasi Aoki
Associate Editor: Daniel Fernandes

Received: 2020.12.18; Accepted: 2021.05.20.

*Correspondence: mainardes@unicentro.br; Tel.: +55-42-36298160 (R.M.M.).

HIGHLIGHTS

- A Taguchi design optimized the development of hesperidin-loaded gliadin nanoparticles.
- A chitosan-coating was added to improve the physical stability of nanoparticles.
- Nanoparticles reduced the hesperidin cytotoxicity over healthy Vero cells.
- Nanoparticles improved the hesperidin cytotoxicity over tumor cells.

Abstract: Hesperidin is a natural compound which is found in citric fruits and presents antitumor and antimicrobial activities. However, the in vivo efficacy of Hesperidin is reduced due to its low oral bioavailability. Protein-based nanoparticles have been applied to improve biological parameters of drugs and natural compounds. Gliadin is a monomeric protein present in wheat. In this study, gliadin-based nanoparticles containing hesperidin were obtained by desolvation technique and a Taguchi orthogonal array design was employed to optimize the formulation. The independent variables were set as concentration of $CaCl_2$ (0.5; 1 or 2%) and stabilizing agent (Pluronic F68, Tween 80 or sodium caseinate). The dependent variables consisted of mean diameter, polydispersity index, zeta potential, and encapsulation efficiency. The results showed significant effects on the dependent variables when 1% $CaCl_2$ and Pluronic F68 were used. The optimized formulation was coated with chitosan to increase the physical stability of the nanoparticles. The final nanoparticles presented a mean diameter of 321 nm and polydispersity index of 0.217, and spherical shape. After coating, the Zeta potential was +21 mV, and the encapsulation efficiency was 73 %. The in vitro release assay showed that about 98% of the drug was released from the nanoparticles after 48 h. Moreover,

the nanoparticles reduced hesperidin cytotoxicity on healthy cells (Vero cells) and improved the cytotoxicity on tumor cells (HeLa, PC-3 and Caco-2 cells). Results showed that the chitosan-coated gliadin nanoparticles are potential carriers for hesperidin delivery for cancer treatment.

Keywords: Protein nanoparticles; Taguchi orthogonal array design; cytotoxicity.

INTRODUCTION

Hesperidin is a flavonoid compound which is found in citrus fruits, as lemon and sweet oranges [1]. Its structure is composed of a flavanone glycoside attached to a rutinosis, forming a β-7-rutinoside of hesperetin (Figure 1), which chemically is 3',5,7-trihydroxy-4'-methoxy flavanone [2]. Hesperidin has shown to have multiple pharmacological activities [1], such as anti-inflammatory, antifungal, antioxidant, antiviral, hypolipidemic, antidiabetic and antitumor [2–4]. Nonetheless, even after a high intake of hesperidin, low concentrations of its metabolites are found in the bloodstream, indicating limited oral bioavailability, which hinders the therapeutic efficacy of the drug [5]. Thus, the improvement of the physicochemical properties of hesperidin through the design of innovative drug delivery carriers to overcome such limitations appears as an important tool. Along these lines, since hesperidin have demonstrated cytotoxicity activity both in vitro and in vivo methodologies [6–12], nanoencapsulation emerge as a tool for the secure, sustained, and efficient release of hesperidin as cancer treatment via oral administration.

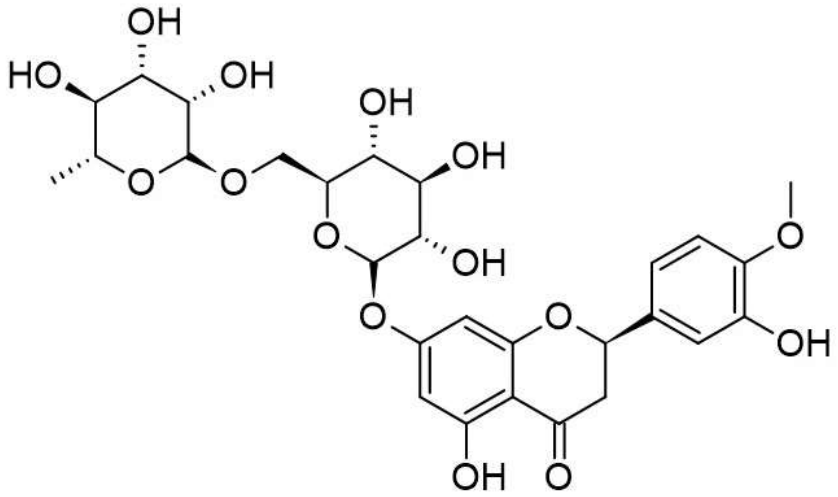

Figure 1. Representation of the chemical structure of hesperidin.

Nanoparticles have been successfully used to improve the oral bioavailability of natural compounds [13]. Among the advantages of the application of nanoparticles in drug delivery, the increased stability in biological fluids, prolonged drug release, improved absorption and biodistribution and increased plasma half-life have been described. These characteristics allow the improvement of the drug bioavailability after oral administration [14]. In the last few years, some studies have been published about hesperidin nanoparticles. Among the produced nanoparticles containing hesperidin are polysaccharide [15,16], nanocrystals [17], inorganic nanoparticles [18–20] nanoemulsions [21–23], liposomes [24], solid lipid nanoparticles [25], nanosuspensions [26], magnetic [27] and protein nanoparticles [11].

Proteins have presented potential applications in the nanoencapsulation of drugs due to their characteristics of biodegradability and biocompatibility, as well as the possibility to modulate the surface of nanoparticles using attaching ligands [28, 29]. Gliadin is one of the main storage proteins present in wheat, classified as a prolamin due to its high content of proline and glutamine, that, together with glutenin, make up a fraction of 80 - 85% of wheat flour, known as gluten [30]. Gliadin presents low solubility in aqueous or neutral saline solutions, because of its high content of nonpolar amino acids, such as glycine and proline, and low amount of ionizable side chain amino acids. Thus, hesperidin presents solubility in hydroalcoholic solutions (70%, v/v), in which its properties of viscoelasticity, foamability and mucoadhesion are observed [31]. By virtue of its characteristics, gliadin has been applied to the nanoencapsulation of compounds for food and pharmaceutical industry [32–34].

Chitosan is a polysaccharide obtained by the deacetylation of chitin naturally found in the body structures of crustaceans and arachnids. It is composed of copolymers of N-acetyl-glucosamine and N-glucosamine units, being a natural alkaline compound that presents good biocompatibility and biodegradability [35,36]. Also, due to its mucoadhesive properties, chitosan is widely employed either as matrix or coat agent for nanoparticles intended for oral administration [36].

In the present study, we developed hesperidin-loaded gliadin nanoparticles and employed a Taguchi orthogonal array design to evaluate the effect of some variables on mean diameter, size distribution, zeta potential and drug encapsulation efficiency. The optimal formulation was coated with chitosan and the in vitro release profile and cytotoxicity on healthy and tumor cells were assessed.

MATERIAL AND METHODS

Materials

Gliadin, hesperidin, low molecular weight Chitosan (50,000–190,000 Da) (75–85% deacetylated), sodium caseinate, MTT (3-(4,5-dimethyl-2-thiazolyl)-2,5-diphenyl- 2H-tetrazolium bromide), fetal bovine serum (FBS), Dulbecco's Modified Eagle Medium (DMEM) were purchased from Sigma-Aldrich® (Missouri, USA). Dimethyl sulfoxide (DMSO), Pluronic F68 and $CaCl_2$ were purchased from Biotec® (Brazil). Ethanol was purchased from FMaia (Brazil). Acetic Acid was purchased from Sigma-Aldrich® (Missouri, USA). Water was purified using a Milli-Q Plus system (Millipore) with a conductivity of 18 MΩ.

Taguchi Orthogonal Array Design

Two variables and their influence on the physicochemical properties of gliadin nanoparticles containing hesperidin were evaluated using Taguchi design employing MINITAB 14.12.0 software (Minitab Inc., State College, PA USA). The independent variables were concentration of $CaCl_2$ in three levels (0.5, 1 or 2%) and the employed surfactant (1% Pluronic F68, 1% Tween 80 or 1% sodium caseinate), while the dependent variables were mean diameter, polydispersity index (PDI), zeta potential and encapsulation efficiency (EE). The applied design required a total of 9 experiments performed in triplicate.

Preparation of gliadin nanoparticles containing hesperidin and chitosan coating

Gliadin nanoparticles containing hesperidin (GLINP-HES) were obtained by the desolvation technique, using the parameters that were optimized through the Taguchi orthogonal design. Briefly, hesperidin (2 mg) and gliadin (30 mg) were solubilized in 70% ethanol. This phase was dropwise added into 9 mL of an aqueous solution containing $CaCl_2$ and the surfactant, using a peristaltic pump with a drip speed of 1 mL/min. The mixture was maintained under agitation for 5 min, the organic solvent was removed by evaporation under vacuum at 37 °C for 20 min and the GLINP-HES were ultracentrifuged at 28,672 g, 15 °C, for 20 min (Z36HK Hermle Wehingen, BH, Germany).

The optimized gliadin nanoparticles containing hesperidin were coated with chitosan (CHGLINP-HES). For this, the nanoparticles obtained after ultracentrifugation (28,672 g, 15 °C, for 20 min) were dispersed into chitosan solution (0.05 % m/v – prepared in 1% acetic acid) and incubated for 1 h at 150 rpm (37°C) in incubator shaker. Then, the nanoparticles were ultracentrifuged (28,672 g, 15 °C, for 20 min) and the pellets were resuspended in water and stored at 8 °C for further analysis.

Mean diameter, size distribution, PDI and zeta potential

The parameters size and PDI of nanoparticles were assessed by dynamic light scattering (DLS) equipment (BIC 90 Plus, Brookhaven Instruments Corp., Holtsville, NY). All measurements were performed in triplicate with a scattering angle of 90° at 25°C and a laser wavelength set at 659 nm. The zeta potential was assessed through a ZetaSizer ZS apparatus (Malvern Instruments Ltd., Worcestershire, UK). The samples were diluted in 1 mM KCl solution and placed in the electrophoretic cell at 25 °C with the application of ± 150 mV.

Encapsulation efficiency (EE)

The EE of hesperidin into nanoparticles was indirectly determined by UV spectrophotometer (UV-1800, Shimadzu Corporation., Ltd., Japan) at 286 nm [2,19]. The sample was the supernatant containing the non-

encapsulated hesperidin resultant of nanoparticles ultracentrifugation. The EE was calculated according to Equation 1:

$$\boldsymbol{EE}\ (\%) = \frac{(\boldsymbol{Total\ amount\ of\ drug - Drug\ amount\ in\ supernatant})}{(\boldsymbol{Total\ amount\ of\ drug})}\ .\mathbf{100} \quad (1)$$

Morphology

The morphology of nanoparticles was examined by scanning electron microscopy (SEM - Hitachi, TM3000 XSTREAM2). A drop of nanoparticle dispersion, after drying, was recovered with colloidal gold under vacuum and analyzed at an accelerating voltage of 10.0 kV to obtain the photomicrographs.

In vitro hesperidin release profile assay

Chitosan-coated gliadin nanoparticles containing 0.3 mg of hesperidin were dispersed in 1 mL of 50 mM phosphate buffered saline (PBS), pH 7.4. The suspension was incubated in a shaker at 37 °C and 150 rpm. At pre-determined times (1, 2, 4, 8, 24 and 48 h), the suspension was centrifuged (20 min at 28,672 g and 25 ºC), and the supernatant was analyzed by UV spectroscopy and the precipitate was suspended in 1 mL of PBS medium and incubated again until next sampling [37]. The cumulative amount of hesperidin released from nanoparticles was calculated according to Equation 2:

$$\boldsymbol{Cumulative\ Release}\ (\%) = \frac{\boldsymbol{Q_1}}{\boldsymbol{Q_0}}.\mathbf{100} \quad (2)$$

Where:
Q_1 is the amount of hesperidin released from nanoparticles at the time (t) and Q_0, the initial amount of hesperidin present in nanoparticles.

Stability studies

The stability of the CHGLINP-HES was evaluated over a period of 120 days. The parameters mean diameter, polydispersity index and zeta potential were determined in samples stored in aqueous suspension in both refrigeration (4 - 10 ºC) and room (22 ± 2 ºC) temperatures. The analyzes were performed in triplicate and a confidence level of 95% ($p<0.05$) was established.

Cytotoxicity assay

The cytotoxicity of the free hesperidin, blank and CHGLINP-HES were evaluated against the following cell lines: Vero (ATCC CCL-81 - normal cells from kidney of an African green monkey, HeLa (ATCC CCL-2 - human cervix adenocarcinoma, PC-3 (ATCC CRL-1435 - human prostate adenocarcinoma, and Caco-2 (ATCC HTB-37 - human colon adenocarcinoma) cells using the (3- [4,5-dimethylthiazol-2-yl] -2,5-diphenyltetrazolium bromide) tetrazolium salt (MTT) reduction cell viability assay. This method is based on the ability of cells to convert the yellow-colored MTT into an insoluble purple compound, called formazan, which occurs when there is integrated mitochondrial capacity. The amount of formazan is determined spectroscopically after solubilization in DMSO. The cell lines were plated at a density of 5 x 10^5 cells/mL in a 96-well cell culture plate for 24 h at 37 °C, under a 5% CO_2 atmosphere. Then, free hesperidin, blank and CHGLINP-HES were added in increasing concentrations (0.1 – 500 µg/mL) for 72 h. After treatment, cells were incubated in the presence of MTT (2 mg/mL) for 4 h at 37 °C. The supernatant was added to DMSO, and with the complete solubilization of the formazan crystals the absorbance reading was carried out at 570 nm in a microplate spectrophotometer (Power Wave XS - Bio-Tek). The percentage that inhibited the absorbance of 50% compared to the control (IC_{50}) was determined by a graphic relating with the concentration of the compounds.

Statistical Analysis

The experiments were conducted in triplicate and the data presented as mean ± standard deviation. Experimental statistics were performed using MINITAB 18 software (Minitab Inc., PA, USA). One-way analysis of variance (ANOVA) with Tukey post-test t was applied to the formulation data and cytotoxicity assay, considering $p < 0.05$.

RESULTS AND DISCUSSION

Design of gliadin nanoparticles and characterization

In this study, the desolvation method was applied to prepare the GLINP-HES and a Taguchi orthogonal array design was performed to analyze the surfactant and $CaCl_2$ concentration influence on the mean diameter, PDI, zeta potential and EE, in search of an optimal and stable formulation. The desolvation method is based on the protein precipitation in the form of nanoparticles when a non-solvent is added to the protein solution under agitation. The presence of a stabilizer is essential to maintain the stability of the formed colloids as well as to help on size reduction and PDI, with good EE, while $CaCl_2$ was applied as precipitation medium. In pre-formulation studies, the nanoparticles without $CaCl_2$ presented very low yield. The results are shown in Table 1.

Table 1. Mean diameter, polydispersity index (PDI), zeta potential and encapsulation efficiency (EE) of hesperidin-loaded gliadin nanoparticles (GLINP-HES) according to the Taguchi design.

Experiment	Mean diameter (nm)	PDI	Zeta potential (mV)	EE (%)
1 (C1,S1)	179.60 ± 23.32	0.25 ± 0.12	-7.43 ± 0.55	50.84 ± 5.06
2 (C1,S2)	177.90 ± 22.55	0.28 ± 0.13	-8.07 ± 0.52	58.02 ± 5.07
3 (C1,S3)	1857.50 ± 337.70	0.53 ± 0.04	-13.10 ± 2.21	87.21 ± 4.71
4 (C2,S1)	226.50 ± 30.97	0.09 ± 0.02	-2.91 ± 0.68	80.11 ± 1.15
5 (C2,S2)	2253.00 ± 262.70	0.69 ± 0.20	-14.90 ± 1.41	49.74 ± 0.83
6 (C2,S3)	1659.50 ± 481.00	0.64 ± 0.09	-11.2 ± 3.11	83.21 ± 0.79
7 (C3,S1)	257.40 ± 25.72	0.16 ± 0.55	-0.21 ± 0.01	55.26 ± 3.01
8 (C3,S2)	1415.60 ± 143.21	0.75 ± 0.18	-14.70 ± 3.23	58.25 ± 8.50
9 (C3,S3)	2591.20 ± 355.80	0.78 ± 0.02	-12.30 ± 2.61	80.04 ± 2.04

Results expressed as mean ± standard deviation (n=3). C1: [$CaCl_2$] = 0.5 %; C2: [$CaCl_2$] = 1.0 %; C3: [$CaCl_2$]= 2.0 %; S1: Pluronic F68; S2: Tween 80; S3: Sodium Caseinate.

As shown, the stabilizer was the most important parameter controlling the mean diameter and PDI, since when the concentration of $CaCl_2$ was maintained, the mean diameter changed according to the stabilizer. The mean diameter ranged from 177 to 2591 nm, whereas the PDI ranged from 0.09 to 0.78. All nanoparticles prepared with Pluronic F68 produced homogeneous and monodispersed gliadin nanoparticles showed better (low size and PDI) results than those composed of sodium caseinate or Tween 80 (except for the formulation 2), and it may be due to their better interaction with gliadin than with other stabilizers. The zeta potential of gliadin nanoparticles ranged from -0.21 to -15 mV, and the nanoparticles composed of Pluronic F68 presented the lowest values (-0.21 to -7.43 mV). The encapsulation efficiency was highly influenced for the stabilizer, since it ranged from 49 to 87%. The highest values were associated with sodium caseinate.

To evaluate the effect of the stabilizer and $CaCl_2$ concentration, graphics of interaction were plotted in Figure 2. It was observed a reduction of mean diameter with Pluronic F68, independent of the $CaCl_2$ concentration (Figure 2A). The ANOVA showed that the variable stabilizer had a significant effect on mean diameter ($p<0.05$), and an interaction with $CaCl_2$ concentration only when it was associated with Tween 80 or sodium caseinate ($p<0.05$). The analysis of PDI (Figure 2B) followed the same pattern. Figure 2C shows the highest zeta potential values obtained with sodium caseinate, independent of the $CaCl_2$ concentration. On the other hand, there was an interaction between 0.5% $CaCl_2$ and both Tween 80 and Pluronic F68 ($p<0.05$). Figure 2D shows the interaction of Pluronic F68 and 1% $CaCl_2$ ($p<0.05$), increasing the EE.

The mean diameter and PDI are the main parameter to be considered for biological application of nanoparticles. Aiming the oral route, nanoparticles smaller than 500 nm are required to pass through the biological barriers, while for tumor targeting, vascular permeability allows the penetration of particles not bigger than 400 nm [38]. PDI is an important indicative of homogeneity of size distribution. Values close to 0 indicate dispersion uniformity and values close to 1 indicate high heterogeneity in particle diameter [38]. The nanoparticles formed with Pluronic F68 presented the lower size and PDI, and it may be due to their better interaction with gliadin than with those occurred with the other stabilizers. In addition, Pluronic F68 produced

homogeneous and monodispersed gliadin nanoparticles. The zeta potential of gliadin nanoparticles was negative, but the values were not greater than -15 mV, since the gliadin isoelectric point is 6.5. The zeta potential is correlated to the nanoparticles suspension stability, as values above ± 30 mV indicate higher stability of particles, as a result of the strong electrostatic repulsion between the nanoparticles [39]. Stabilizers are used to facilitate the particle formation, contributing to decrease the mean diameter, and also to increase the physical stability of the particles [40]. Pluronic F68, Tween 80 and sodium caseinate are non-ionic stabilizers, thus, they do not contribute to the zeta potential increase, and the final nanoparticles were difficult to disperse in water, remaining agglomerated. The stabilizer influenced the encapsulation efficiency, and sodium caseinate originated nanoparticles with higher encapsulation efficiency, probably as a result of the higher mean diameter of these nanoparticles. Thus, from the results of the Taguchi design and graphics of interaction, an optimal GLINP-HES formulation was found to be composed of Pluronic F68 and 1% $CaCl_2$ (Experiment 4).

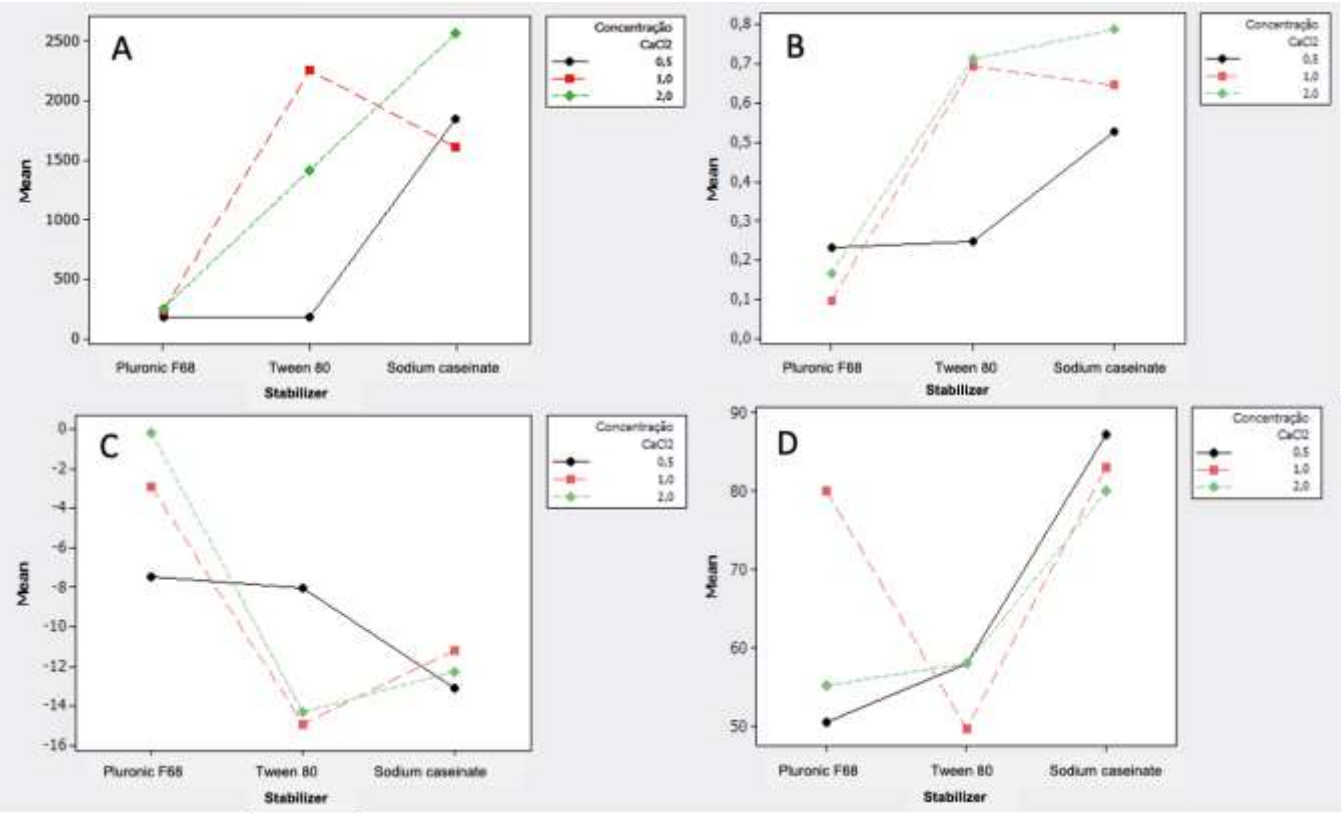

Figure 2. Interaction plots for the experimental Taguchi design demonstrating data about (A) mean diameter, (B) polydispersity index, (C) zeta potential and (D) encapsulation efficiency.

Chitosan coating

Due to the difficult of redispersion presented by GLINP-HES, the optimized formulation was subjected to chitosan coating to increase the colloidal stability, improve their redispersion and ameliorate them for further oral delivery. Table 2 shows the characteristics of gliadin nanoparticles before and after chitosan coating.

Table 2. Mean size, polydispersity index (PDI), zeta potential and entrapment efficiency (EE) of uncoated (GLINP-HES) and chitosan-coated gliadin nanoparticles containing hesperidin (CHGLINP-HES) (n=3).

Nanoparticles	Mean size (nm)	PDI	Zeta potential (mV)	EE (%)
GLINP-HES	226.50 ± 30.97[a]	0.09 ± 0.02[a]	-2.91 ± 0.68[a]	80.11 ± 1.15[a]
CHGLINP-HES	321.40 ± 39.60[b]	0.217 ± 0.06[b]	+21.40 ± 2.07[b]	73.10 ± 2.42[b]

[a, b] Different letters present statistical difference ($p < 0.05$). (One-way ANOVA, Tukey post-test t), analyzed by column.

The nanoparticles mean diameter increased after chitosan coating ($p<0.05$), which was expected since chitosan was applied after gliadin nanoparticles formation. In another study of our group, chitosan coating increased the mean diameter of zein nanoparticles from 220 to 382 nm [37]. A similar study suggested the presence of an external corona after covering nanoparticles with chitosan [41].

The zeta potential analysis performed after coating demonstrated a chemical modification occurred on the nanoparticles surface. The zeta potential changed from negative to positive, supporting the presence of chitosan moieties covering the nanoparticles. It occurs due to the positive-charged amino groups of chitosan interaction with negative-charged gliadin nanoparticles surface, through electrostatic interaction [42]. Besides improving the colloidal stability, the positive zeta potential can result in the better interaction of nanoparticles with biological mucosa. Positively charged nanoparticles interact electrostatically with negatively charged mucus layer, increasing the retention time at the sites of absorption, thereby improving the absorption and consequently the bioavailability of the drug-loaded [43]. In another work, we showed the important role of chitosan coating in increasing the permeability of PLGA nanoparticles in a cell model containing mucus-producing goblet cells, enterocytes and M cells (Caco-2/HT29-MTX/Raji B co-culture) [44]. On the other hand, due to incubation with chitosan, some hesperidin moieties adsorbed into the gliadin nanoparticles surface suffered desorption to medium, resulting in a slight decrease in encapsulation efficiency ($p<0.05$).

SEM analysis of nanoparticles before and after chitosan coating (Figure 3A and 3B, respectively) evidenced a slight spherical shape of nanoparticles, and confirmed the mean diameter data obtained by dynamic light scattering. Although the nanoparticles presented some aggregates, possibly due to the sample-drying process, the uncoated nanoparticles were more aggregated and disform compared to chitosan coated ones.

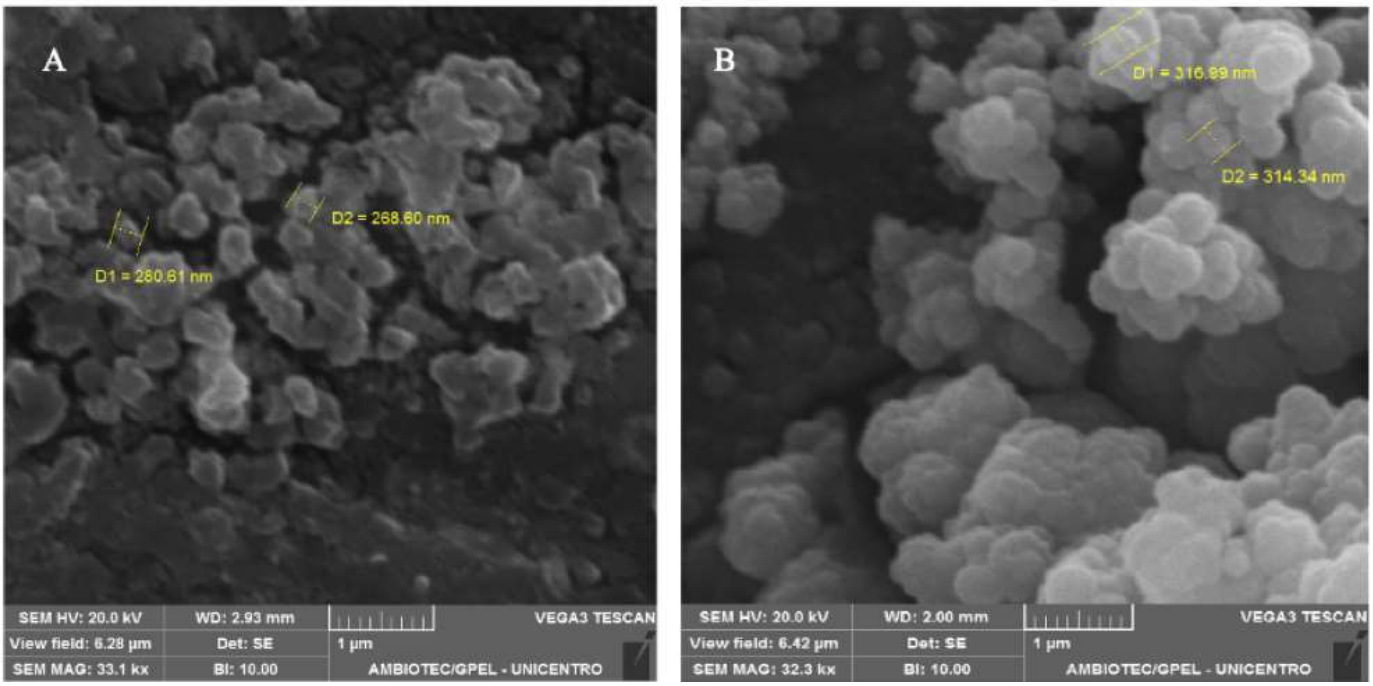

Figure 3. Scanning electron microscopy (SEM) photomicrographs corresponding to: uncoated (A) and chitosan-coated (B) gliadin nanoparticles containing hesperidin.

In vitro release profile

The in vitro release profile showed the sustained release of hesperidin from nanoparticles over 48 h (Figure 4). A biphasic profile was observed, with an initial burst effect during the first 4 h, releasing about 37% of hesperidin, followed by a sustained release for 48 h, releasing almost all the drug remained. About 98% of the drug was released after 48 h. The slow release can be attributed to the efficient retention capability of chitosan-coated gliadin nanoparticles.

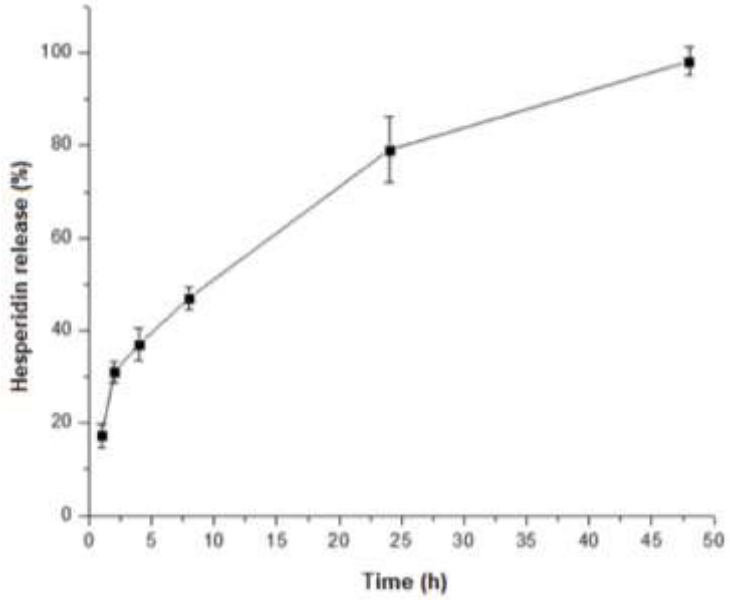

Figure 4. In vitro release profile of hesperidin from chitosan-coated gliadin nanoparticles in PBS (50 mM, pH 7.4).

Due to its cationic character, chitosan has been widely applied as coating agent to enhance controlled drug release [45]. Khan and coauthors have proved the chitosan capacity to retard drug release from hydrogel [45]. According to Shao and coauthors study, nanoparticles containing chitosan were able to limited drug diffusion [46]. Although the chitosan ability to improve controlled drug release has been proved [36], further studies should be developed to evaluate the role of chitosan as coating material for gliadin nanoparticles. The drug delivery modulation achieved by nanostructured systems has shown to be advantageous, since the fluctuation in plasma concentration is reduced, tissue drug levels are maintained, and the intervals between dose can be spaced out, reducing the side effects caused by a rapid drug release [47].

Stability studies

The stability of CHGLINP-HES was evaluated through the mean diameter, polydispersity index and zeta potential measurements. The samples were maintained in aqueous solution for 120 days. Figure 5 presents the results obtained for CHGLINP-HES stability.

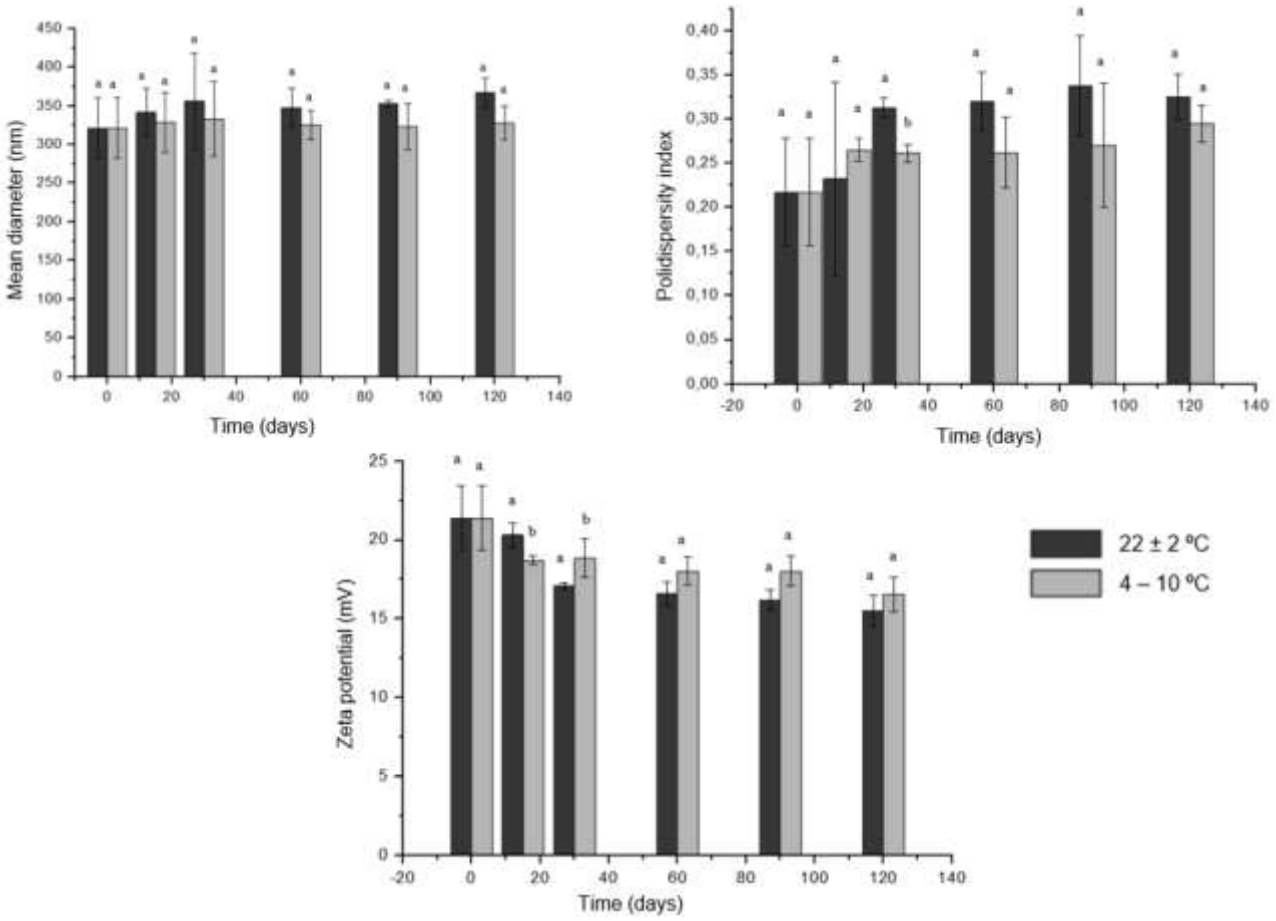

Figure 5. Mean diameter, PDI and zeta potential values for the stability study of hesperidin from chitosan-coated gliadin nanoparticles. ([a, b] Different letters present statistical difference ($p < 0.05$). (One-way ANOVA, Tukey post-test t).

The particle size of the hesperidin-loaded chitosan coated gliadin nanoparticles remained stable for 120 days after preparation ($p<0.05$). On the same period, the polydispersity index had increased after 20 days of storage at room temperature, while refrigerated samples kept the homogeneity of the particles. Although the PDI raised over the next days, specially at room temperature, the increase was not significant ($p<0.05$). Likewise, the superficial charge of the nanoparticles continued high over the time evaluated. Even though there was a decrease on zeta potential values, the changes were not significant ($p<0.05$).

Cytotoxicity assay

The cytotoxicity of the hesperidin-loaded chitosan coated gliadin nanoparticles (CSGLINP-HES) was evaluated in a model of healthy (Vero) and tumor (HeLa, PC-3 and Caco-2) cells, and the cell viability and IC_{50} were compared to blank nanoparticles and free hesperidin. Table 3 shows IC_{50} and Figure 6 presents cell viability comparison after 72-h incubation with the studied samples.

Table 3. Cytotoxicity evaluation in terms of IC_{50} values of free hesperidin, blank nanoparticles, and hesperidin-loaded chitosan-coated nanoparticles (CSGLINP-HES) against healthy (Vero) cells, and tumor (HeLa, PC-3, and Caco-2) cells, at 72h.

Cell line	IC_{50} (µg/mL)		
	Free Hesperidin	CSGLINP-HES	Blank nanoparticles
Vero	230.83 ± 20.05	> 1000	> 1000
HeLa	70.44 ± 7.72	16 ± 1.61	159.33 ± 12.10
PC-3	179.05 ± 3.68	21.62 ± 1.84	126.67 ± 14.05
Caco-2	265.53 ± 17.56	164.87 ± 14.72	674.45 ± 62.03

Most synthetic chemotherapeutic agents for cancer treatment affect both tumor and healthy cells, leading to higher chances of side effects. On the other hand, naturally occurred bioactive compounds proved to be more selective to cancer sites [11]. In this study, the cytotoxic effect of CSGLINP-HES on Vero cells was evaluate as a model for healthy cells. A reduction of the cell viability was observed with blank and CSGLINP-HES in 50 and 100 µg/mL ($p<0.05$), as shown in Figure 6A. However, in higher drug concentrations, free hesperidin was significatively more cytotoxic than blank and CSGLINP-HES ($p<0.05$). The IC_{50} of free hesperidin was at least 5-fold less than blank and hesperidin-loaded nanoparticles. The results show that nanoencapsulation reduces the cytotoxicity of hesperidin in this model of healthy cells.

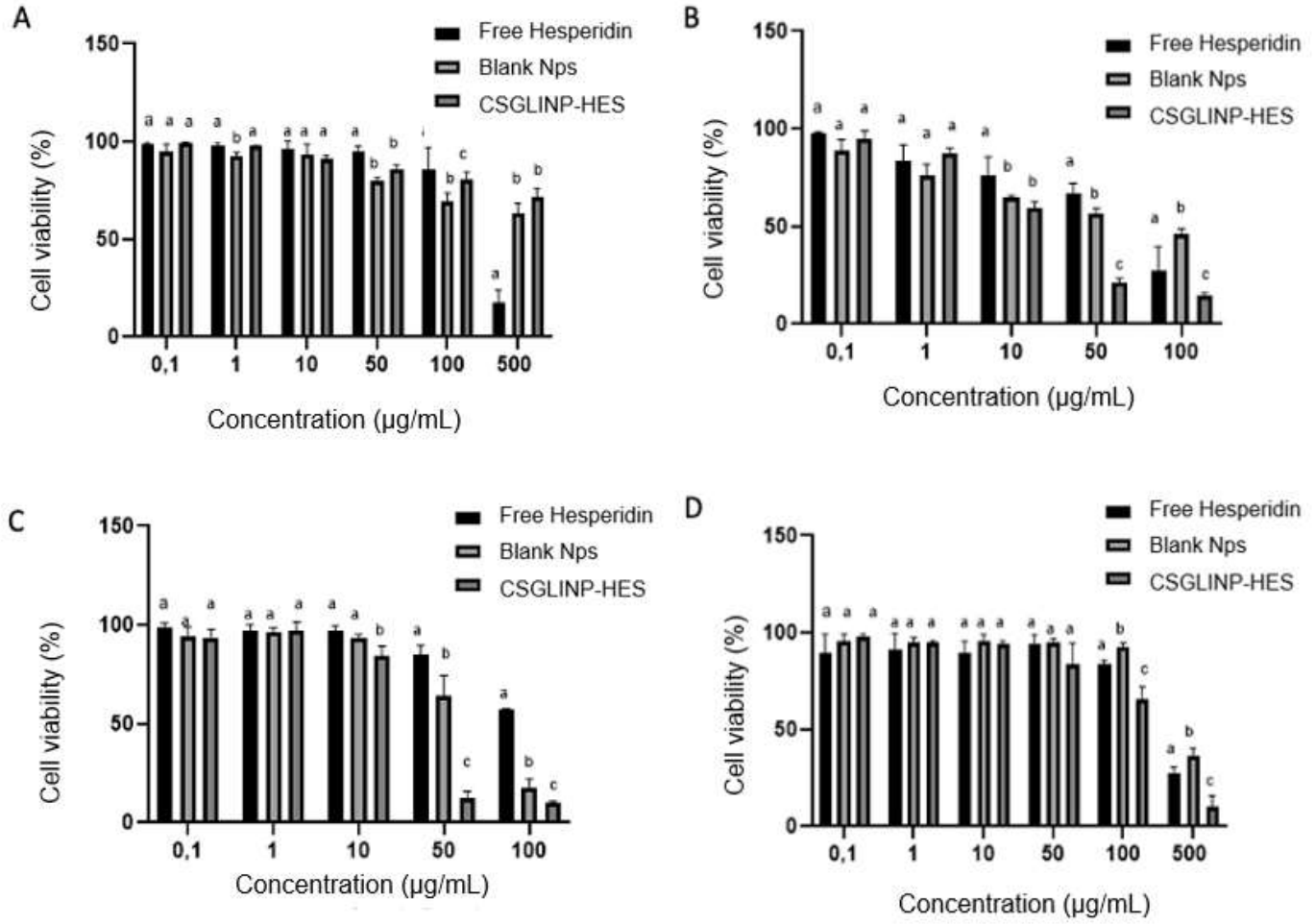

Figure 6. Cell viability of Vero (A), HeLa (B), PC-3 (C), and Caco-2 cells (D) against hesperidin-loaded chitosan-coated gliadin nanoparticles (CSGLINP-HES) compared to blank nanoparticles and free hesperidin, at 72h. ([a, b, c] Different letters present statistical difference ($p<0.05$). (GraphPad Prism 8; One ANOVA; Post Tukey).

On the contrary, in HeLa cells the CSGLINP-HES were significantly more cytotoxic than free hesperidin in all evaluated concentrations ($p<0.05$) (Figure 6B). The IC_{50} of CSGLINP-HES was 4.5-fold lower than free hesperidin, indicating its higher efficacy, and the IC_{50} of blank nanoparticles were 2.2-fold higher than from free hesperidin. Bartoszewski and coauthors (2014) studied the effect of hesperidin against HeLa cells and stated that the drug led to apoptosis by extrinsic pathway, since an increase of mRNA levels was observed in death receptors of apoptosis [7]. In the same manner, Ferreira de Oliveira and coauthors (2020) found out a that hesperidin was able to inhibit cell cycle transition in HeLa cells and also induce intracellular oxidation [47]. Consonantly, Stanisic and coauthors (2018) observed hesperidin capacity to increase by three times the calcium concentration in the cytoplasm of HeLa cells, promoting mitochondrial dysfunction that leads to apoptosis [48].

The CSGLINP-HES were also evaluated against PC-3 prostate cancer cells. As Figure 6C presents, 10 µg/mL of CSGLINP-HES were more efficient than free hesperidin to reduce the cell viability ($p<0.05$). Notably, blank nanoparticles also showed to be more cytotoxic than free drug ($p<0.05$), in 50 and 100 µg/mL. The IC_{50} of hesperidin nanoparticles was 8.3-fold lower than free hesperidin, and 1.5-fold lower than blank nanoparticles, indicating its higher cytotoxic efficacy. Lewinska and coauthors (2014) explained thar flavonoid

glycosides, such as hesperidin, are DNA hypomethylating agents capable of inducing gene expression changes and increased superoxide production in vitro, leading to apoptosis [49]. Moreover, Lau (2010) results showed that hesperidin was efficient in inhibit PC3 cells viability without significant effect on healthy cells [50].

Caco-2 cells are considered a “golden standard” for in vitro models of intestine cancers [51]. In our findings, CSGLINP-HES in a concentration starting from 100 µg/mL showed to be more cytotoxic than free hesperidin ($p<0.05$). The IC_{50} was 1.6-fold lower than free hesperidin, and blank nanoparticles presented 2.6-fold higher than free hesperidin, as presented in Figure 6D. According to Kobayashi & Konishi (2008), hesperidin is absorbed in the intestine by active transport and transcellular passive diffusion [52]. Andrade et al. (2017) noted that hesperidin inhibits fructose’s absorption for Caco-2 cells [55]. Regarding to nanotechnology applied to cancer treatment, some studies have demonstrated the higher permeability of hesperidin nanoparticles to Caco-2 cells [10,53].

In this study, CSGLINP-HES were more effective in reducing cell viability of the three evaluated tumor cell lines compared to the non-encapsulated compound. Presumably, the positive charge associated to the produced nanoparticles increased the interaction and their uptake by negatively charged tumor cells. Also, the higher efficacy of CSGLINP-HES can be inferred by the efficiency of the nanoparticles per se plus the drug activity, and their activity may be a result of a synergistic effect. Studies have shown that chitosan nanoparticles present antitumor activity due to membrane disrupting and apoptosis-inducing activities [54]. The reason for the low cytotoxicity of CSGLINP-HES in Vero cells may be due to the intracellular pH. When compared to healthy cells, tumor cells present abnormal acid intracellular pH [11]. Consequently, in acid pH, chitosan and gliadin become protonates and the drug release is facilitated, leading to higher selectivity for tumor cells than for healthy cells, an important requirement for cancer therapy [11]. These characteristics show the potential of the chitosan-coated gliadin nanoparticles to be investigated as a new approach for cancer treatment, allowing oral administration of chemotherapeutic compounds with reduced side effects.

CONCLUSION

In this study, the desolvation method was successfully applied to obtain gliadin nanoparticles containing hesperidin and a Taguchi design allowed the formulation optimization. The chitosan-coated gliadin nanoparticles promoted a prolonged drug release in a biphasic profile and significantly reduced the hesperidin cytotoxicity against health cells, while inhibited tumor cells more efficiently than free drug. Our results demonstrated the potential of the chitosan-coated gliadin nanoparticles loaded with hesperidin as possible anticancer agent.

Funding: This research was funded by Coordenação de Aperfeiçoamento de Pessoal de Nível Superior (CAPES-Brazil) Financial code 001, financiadora de Estudos e Projetos (FINEP-Brazil), Conselho Nacional de Desenvolvimento Científico e Tecnológico (CNPq-Brazil – proc 313800/2018-9) and PRONEX/Fundação Araucária (Brazil).
Conflicts of Interest: The authors declare no conflict of interest.

REFERENCES

1. Knekt P, Kumpulainen J, Järvinen R, Rissanen H, Heliövaara M, Reunanen A, et al. Flavonoid intake and risk of chronic diseases. 560 Am J Clin Nutr. 2002;76(March):560–8.
2. Garg A, Garg S, Zaneveld LJD, Singla AK. Chemistry and Pharmacology of The Citrus Bioflavonoid Hesperidin. Phytother Res. 2001;15(August):655–69.
3. Benavente-Garcia O, CastilloO J. Update on Uses and Properties of Citrus Flavonoids : New Findings in Anticancer , Cardiovascular , and Anti-inflammatory Activity. J Agric Food Chem 2008,. 2008;56:6185–205.
4. Roohbakhsh A, Parhiz H, Soltani F, Rezaee R, Iranshahi M. Neuropharmacological properties and pharmacokinetics of the citrus fl avonoids hesperidin and hesperetin — A mini-review. Life Sci [Internet]. 2014;113(1–2):1–6. Available from: http://dx.doi.org/10.1016/j.lfs.2014.07.029
5. Manach C, Morand C, Re C. Bioavailability in humans of the flavanones hesperidin and narirutin after the ingestion of two doses of orange juice. Eur J Clin Nutr. 2003;57:235–42.
6. Andrade N, Araújo JR, Correia-Branco A, Carletti J V., Martel F. Effect of dietary polyphenols on fructose uptake by human intestinal epithelial (Caco-2) cells. J Funct Foods [Internet]. 2017;36:429–39. Available from: http://dx.doi.org/10.1016/j.jff.2017.07.032
7. Bartoszewski R, Hering A, Marszałł M, Hajduk JS, Bartoszewska S, Kapoor N, et al. Mangiferin Has an Additive Effect on the Apoptotic Properties of Hesperidin in Cyclopia sp . Tea Extracts. PLoS One. 2014;9(3):1–12.

8. Cilla A, Rodrigo MJ, Zacarías L, De Ancos B, Sánchez-Moreno C, Barberá R, et al. Protective effect of bioaccessible fractions of citrus fruit pulps against H2O2-induced oxidative stress in Caco-2 cells. Food Res Int [Internet]. 2018;103(October 2017):335–44. Available from: http://dx.doi.org/10.1016/j.foodres.2017.10.066
9. Cincin ZB, Kiran B, Baran Y, Cakmakoglu B. Hesperidin promotes programmed cell death by downregulation of nongenomic estrogen receptor signalling pathway in endometrial cancer cells. Biomed Pharmacother [Internet]. 2018;103(April):336–45. Available from: https://doi.org/10.1016/j.biopha.2018.04.020
10. Uchiyama H, Tozuka Y, Asamoto F, Takeuchi H. α-Glucosyl hesperidin induced an improvement in the bioavailability of pranlukast hemihydrate using high-pressure homogenization. Int J Pharm [Internet]. 2011;410(1–2):114–7. Available from: http://dx.doi.org/10.1016/j.ijpharm.2011.03.017
11. Uma Maheswari P, Muthappa R, Bindhya KP, Meera Sheriffa Begum KM. Evaluation of folic acid functionalized BSA-CaFe2O4 nanohybrid carrier for the controlled delivery of natural cytotoxic drugs hesperidin and eugenol. J Drug Deliv Sci Technol [Internet]. 2021;61(September):102105. Available from: https://doi.org/10.1016/j.jddst.2020.102105
12. Yang Y, Bai L, Li X, Xiong J, Xu P, Guo C, et al. Transport of active flavonoids, based on cytotoxicity and lipophilicity: An evaluation using the blood-brain barrier cell and Caco-2 cell models. Toxicol Vitr [Internet]. 2014;28(3):388–96. Available from: http://dx.doi.org/10.1016/j.tiv.2013.12.002
13. Watkins R, Zhang C, Davis RM, Xu B. Natural product-based nanomedicine : recent advances and issues. Int J Nanomedicine. 2015;10:6055–74.
14. Gelperina S, Kisich K, Iseman MD, Heifets L. The Potential Advantages of Nanoparticle Drug Delivery Systems in Chemotherapy of Tuberculosis. Am J Respir Crit Care Med. 2005;172:1487–90.
15. Bagher Z, Ehterami A, Safdel MH, Khastar H, Semiari H, Asefnejad A, et al. Wound healing with alginate/chitosan hydrogel containing hesperidin in rat model. J Drug Deliv Sci Technol [Internet]. 2020;55:101379. Available from: https://doi.org/10.1016/j.jddst.2019.101379
16. Tsirigotis-Maniecka M, Gancarz R, Wilk KA. Polysaccharide hydrogel particles for enhanced delivery of hesperidin: Fabrication, characterization and in vitro evaluation. Colloids Surfaces A Physicochem Eng Asp [Internet]. 2017;532(February):48–56. Available from: http://dx.doi.org/10.1016/j.colsurfa.2017.07.001
17. Praveen KH, Prasad AS. Hesperidin mediated synthesis, structure and optical emission analysis on nanocrystalline CuO. Mater Today Proc [Internet]. 2020;41(xxxx):520–4. Available from: https://doi.org/10.1016/j.matpr.2020.05.237
18. Liu J, Ma X, LingWang. Modulating effect of graphine oxide loaded hesperidin nanocomposite on the 1,2-dimethylhydrazine provoked colon carcinogenesis in rats via inhibiting the iNOS and COX-2 pathways. Arab J Chem [Internet]. 2020;13(8):6708–23. Available from: https://doi.org/10.1016/j.arabjc.2020.06.025
19. Owoseni-Fagbenro KA, Saifullah S, Imran M, Perveen S, Rao K, Fasina TM, et al. Egg proteins stabilized green silver nanoparticles as delivery system for hesperidin enhanced bactericidal potential against resistant S. aureus. J Drug Deliv Sci Technol [Internet]. 2019;50(January):347–54. Available from: https://doi.org/10.1016/j.jddst.2019.02.002
20. Yang Z, Yang H, Dong X, Pu M, Ji F. Hesperidin loaded Zn2+@ SA/PCT nanocomposites inhibit the proliferation and induces the apoptosis in colon cancer cells (HCT116) through the enhancement of pro-apoptotic protein expressions. J Photochem Photobiol B Biol [Internet]. 2020;204(2019 December):111767. Available from: https://doi.org/10.1016/j.jphotobiol.2019.111767
21. Dammak I, Sobral PJ do A. Formulation optimization of lecithin-enhanced pickering emulsions stabilized by chitosan nanoparticles for hesperidin encapsulation. J Food Eng [Internet]. 2018;229:2–11. Available from: https://doi.org/10.1016/j.jfoodeng.2017.11.001
22. Liao Y, Zhong L, Liu L, Xie L, Tang H, Zhang L, et al. Comparison of surfactants at solubilizing, forming and stabilizing nanoemulsion of hesperidin. J Food Eng [Internet]. 2020;281(December 2019):110000. Available from: https://doi.org/10.1016/j.jfoodeng.2020.110000
23. Wei Z, Cheng Y, Zhu J, Huang Q. Genipin-crosslinked ovotransferrin particle-stabilized Pickering emulsions as delivery vehicles for hesperidin. Food Hydrocoll [Internet]. 2019;94(February):561–73. Available from: https://doi.org/10.1016/j.foodhyd.2019.04.008
24. Morsy MA, Nair AB. Prevention of rat liver fibrosis by selective targeting of hepatic stellate cells using hesperidin carriers. Int J Pharm [Internet]. 2018;552(1–2):241–50. Available from: https://doi.org/10.1016/j.ijpharm.2018.10.003
25. Saad S, Ahmad I, Kawish SM, Khan UA, Ahmad FJ, Ali A, et al. Improved cardioprotective effects of hesperidin solid lipid nanoparticles prepared by supercritical antisolvent technology. Colloids Surfaces B Biointerfaces [Internet]. 2020;187(August):110628. Available from: https://doi.org/10.1016/j.colsurfb.2019.110628

26. Long J, Song J, Zhang X, Deng M, Xie L, Zhang L, et al. Tea saponins as natural stabilizers for the production of hesperidin nanosuspensions. Int J Pharm [Internet]. 2020;583(March):119406. Available from: https://doi.org/10.1016/j.ijpharm.2020.119406
27. Purushothaman BK, Maheswari U, Begum MS. Magnetic casein-CaFe2O4 nanohybrid carrier conjugated with progesterone for enhanced cytotoxicity of citrus peel derived hesperidin drug towards breast and ovarian cancer. Int J Biol Macromol [Internet]. 2020;151:293–304. Available from: https://doi.org/10.1016/j.ijbiomac.2020.02.172
28. Lohcharoenkal W, Wang L, Chen YC, Rojanasakul Y. Protein Nanoparticles as Drug Delivery Carriers for Cancer Therapy. Biomed Res Int. 2014;2014:1–12.
29. Weber C, Coester C, Kreuter J, Langer K. Desolvation process and surface characterisation of protein nanoparticles. Int J Pharm 194. 2000;194:91–102.
30. Delcour JA, Joye IJ, Pareyt B, Wilderjans E, Brijs K, Lagrain B. Wheat Gluten Functionality as a Quality Determinant in Cereal-Based Food Products. Annu Rev Food Sci Technol. 2012;3:469–92.
31. Jespersen BM, Munck L. Cereals and Cereal Products. In: Infrared Spectroscopy for Food Quality Analysis and Control. Elsevier Inc.; 2009. p. 275–319.
32. Jahanshahi M, Babaei Z. Protein nanoparticle : A unique system as drug delivery vehicles. African J Biotechnol. 2008;7(25):4926–34.
33. Banc A, Desbat B, Renard D, Popineau Y, Navailles L. Structure and Orientation Changes of ω - and γ -Gliadins at the Air - Water Interface : A PM - IRRAS Spectroscopy and Brewster Angle Microscopy Study. Langmuir. 2007;23(14):13066–75.
34. Arangoa MA, Campanero MA, Renedo MJ, Ponchel G, Irache JM. Gliadin Nanoparticles as Carriers for the Oral Administration of Lipophilic Drugs . Relationships between Bioadhesion and Pharmacokinetics. 2001;18(11):0–6.
35. De Pinho Neves AL, Milioli CC, Müller L, Riella HG, Kuhnen NC, Stulzer HK, et al. Factorial design as tool in chitosan nanoparticles development by ionic gelation technique. Colloids Surfaces A Physicochem Eng Asp [Internet]. 2014;445(2014):34–9. Available from: http://dx.doi.org/10.1016/j.colsurfa.2013.12.058
36. Yu S, Xu X, Feng J, Liu M, Hu K. Chitosan and Chitosan Coating Nanoparticles for the Treatment of Brain Disease. Int J Pharm [Internet]. 2019; Available from: https://doi.org/10.1016/j.ijpharm.2019.02.012
37. Pauluk D, Padilha AK, Khalil NM, Mainardes RM. Chitosan-coated zein nanoparticles for oral delivery of resveratrol: Formation, characterization, stability, mucoadhesive properties and antioxidant activity. Food Hydrocoll. 2019;94:411–7.
38. Avadi MR, Sadeghi AMM, Mohammadpour N, Abedin S, Atyabi F, Dinarvand R, et al. Preparation and characterization of insulin nanoparticles using chitosan and Arabic gum with ionic gelation method. Nanomedicine Nanotechnology, Biol Med. 2010;6(1).
39. Grobelny J, Nmaboodiri P, Kim D, Hackley VA, Cook RF. Size Measurement of Nanoparticles Using Atomic Force Microscopy. Methods Mol Biol. 2011;697(January):71–82.
40. Joye IJ, Nelis VA, Mcclements DJ. Gliadin-based nanoparticles : Fabrication and stability of food-grade colloidal delivery systems. Food Hydrocoll [Internet]. 2015;44:86–93. Available from: http://dx.doi.org/10.1016/j.foodhyd.2014.09.008
41. Hidalgo S, Molina-mateo D, Escobedo P, Zarate R V, Fierro A, Pérez EG, et al. Characterization of a novel Drosophila SERT mutant : insights on the contribution of the serotonin neural system to behaviors. ACS Chem Neurosci. 2017;
42. Li J, Hwang I, Chen X, Jin H. Effects of chitosan coating on curcumin loaded nano-emulsion : Study on stability and in vitro digestibility. Food Hydrocoll [Internet]. 2016;60:138–47. Available from: http://dx.doi.org/10.1016/j.foodhyd.2016.03.016
43. Andreani T, Miziara L, Lorenzón EN, Luiza A, Souza R De, Kiill CP, et al. Effect of mucoadhesive polymers on the in vitro performance of insulin-loaded silica nanoparticles : Interactions with mucin and biomembrane models. Eur J Pharm Biopharm [Internet]. 2015;(April). Available from: http://dx.doi.org/10.1016/j.ejpb.2015.03.027
44. Lima IA de, Khalil NM, Tominaga TT, Lechanteur A, Sarmento B, Mainardes RM. Mucoadhesive chitosan-coated PLGA nanoparticles for oral delivery of ferulic acid. Artif Cells, Nanomedicine Biotechnol [Internet]. 2018;46(sup2):993–1002. Available from: https://doi.org/10.1080/21691401.2018.1477788
45. Khan A, Aqil M, Imam SS, Ahad A, Sultana Y, Ali A, et al. Temozolomide loaded nano lipid based chitosan hydrogel for nose to brain delivery: Characterization, nasal absorption, histopathology and cell line study. Biol Macromol [Internet]. 2018;(2017). Available from: https://doi.org/10.1016/j.ijbiomac.2018.05.079
46. Shao Y, Wu C, Wu T, Li Y, Chen S, Yuan C, et al. Eugenol-chitosan nanoemulsions by ultrasound-mediated emulsi fi cation : Formulation , characterization and antimicrobial activity. Carbohydr Polym [Internet]. 2018;193(December 2017):144–52. Available from: https://doi.org/10.1016/j.carbpol.2018.03.101

47. Ferreira de Oliveira JMP, Santos C, Fernandes E. Therapeutic potential of hesperidin and its aglycone hesperetin: Cell cycle regulation and apoptosis induction in cancer models. Phytomedicine [Internet]. 2020;73(February):152887. Available from: https://doi.org/10.1016/j.phymed.2019.152887
48. Stanisic D, Costa AF, Fávaro WJ, Tasic L, Seabra AB, Durán N. Anticancer Activities of Hesperidin and Hesperetin In vivo and their Potentiality against Bladder Cancer. J Nanomed Nanotechnol. 2018;9(5):1–6.
49. Lewinska A, Siwak J, Rzeszutek I, Wnuk M. Diosmin induces genotoxicity and apoptosis in DU145 prostate cancer cell line. Toxicol Vitr [Internet]. 2014;29(3):417–25. Available from: http://dx.doi.org/10.1016/j.tiv.2014.12.005
50. Lau Y-K. A novel anti-cancer effect of hesperidin: reversion of epithelial mesenchymal transition in human prostate cancer cells. In: American Association for Cancer Research. Washington, DC: AACR; 2010. p. 100–1.
51. Shen C, Chen R, Qian Z, Meng X, Hu T, Li Y, et al. Intestinal absorption mechanisms of MTBH, a novel hesperetin derivative, in Caco-2 cells, and potential involvement of monocarboxylate transporter 1 and multidrug resistance protein 2. Eur J Pharm Sci [Internet]. 2015;78:214–24. Available from: http://dx.doi.org/10.1016/j.ejps.2015.07.022
52. Kobayashi S, Konishi Y. Transepithelial transport of flavanone in intestinal Caco-2 cell monolayers. Biochem Biophys Res Commun. 2008;368(1):23–9.
53. Tozuka Y, Imono M, Uchiyama H, Takeuchi H. A novel application of α-glucosyl hesperidin for nanoparticle formation of active pharmaceutical ingredients by dry grinding. Eur J Pharm Biopharm [Internet]. 2011;79(3):559–65. Available from: http://dx.doi.org/10.1016/j.ejpb.2011.07.006
54. Oberemko A, Salaberria AM, Saule R, Saulis G, Kaya M. Physicochemical and in vitro cytotoxic properties of chitosan from mushroom species (Boletus bovinus and Laccaria laccata). Carbohydr Polym [Internet]. 2019;221(April):1–9. Available from: https://doi.org/10.1016/j.carbpol.2019.05.073
55. Andrade N, Araújo JR, Correia-Branco A, Carletti JV, Martel F. Effect of dietary polyphenols on fructose uptake by human intestinal epithelial (Caco-2) cells. Journal of Functional Foods, v. 36, p. 429–439, 2017. Available from: https:// 10.1016/j.jff.2017.07.032